Mine Water Environ (2013) 32:152–167
DOI 10.1007/s10230-013-0225-9

TECHNICAL ARTICLE

Assessment of Phosphate Limestone Wastes as a Component of a Store-and-Release Cover in a Semiarid Climate

Bruno Bossé · Bruno Bussière · Rachid Hakkou · Abdelkabir Maqsoud · Mostafa Benzaazoua

Received: 16 August 2012 / Accepted: 1 March 2013 / Published online: 20 March 2013

Abstract In a semiarid climate where the annual precipitation is low and the evaporation rate is high, contaminated drainage production from mine tailings can be controlled by reducing water infiltration. Store-and-release covers that use capillary barrier effects can prevent water percolation by storage and evaporation (or evapotranspiration) during wet and dry climatic periods. In Morocco, sedimentary phosphate mines are located close to contaminated sites, which includes the abandoned Kettara mine. This mine site generates highly contaminated acid rock drainage (ARD) with negative impacts on its surrounding area. In order to validate if phosphate mine wastes can be used as cover material to reclaim the Kettara site, instrumented test columns were exposed to field conditions and tested for a period of one and a half years. Under natural conditions, more than 94 % of the total net infiltration (246.5 mm) was released to the atmosphere by evaporation. Preliminary tests showed that the studied scenarios can limit deep water infiltration even during extreme simulated rainfall (155 mm/d) and could be used to efficiently control contaminated drainage in a semiarid climate.

B. Bossé (✉) · B. Bussière · A. Maqsoud · M. Benzaazoua
Research Institute on Mines and the Environment, Univ du Québec en Abitibi-Témiscamingue, 445 Boul. de l'Université, Rouyn-Noranda, Québec J9X 5E4, Canada
e-mail: bruno.bosse@uqat.ca

B. Bossé · R. Hakkou · M. Benzaazoua
IDRC (Canada) Research Chair in Management and Stabilization of Mining and Industrial Wastes, Univ Cadi Ayyad, Marrakech, Morocco

R. Hakkou
LCME, Faculté des Sciences et Techniques, Univ Cadi Ayyad, BP 549, 40000 Marrakech, Morocco

Keywords Acid rock drainage · Store-and-release cover · Kettara mine site · Mine site reclamation

Introduction

Engineered cover systems are widely used to limit water infiltration into waste disposal areas that contain hazardous, municipal, industrial, mining or radioactive wastes (e.g. Albright et al. 2010; Daniel and Koerner 2007; Hauser 2008). These cover systems, usually made of specific barrier layers, can be divided into two main categories: conventional cover systems (e.g. compacted clay layers, combined or not with a geomembrane liner) and alternative cover systems that use the physical process of evaporation to control water infiltration. Recent studies have shown that these alternative systems are efficient in arid or semiarid climates and perform as well or even better than conventional systems that use low saturated hydraulic conductivity materials (e.g. Albright et al. 2004; Benson et al. 2002; Dwyer 2003; Gee et al. 2006; Morris and Stormont 1997; Rock et al. 2012). These alternative cover systems are known in the literature as evapotranspiration (ET) covers (e.g. Barnswell and Dwyer 2011; Dwyer 2003; EPA 2011, 2012; Madalinski et al. 2003; McGuire et al. 2009; Nyhan 2005; Scanlon et al. 2005), water balance covers (e.g. Albright et al. 2010; Benson et al. 2007), and store-and-release (SR) covers (e.g. O'Kane et al. 1998; Williams et al. 2006), which is the term used in this paper.

SR covers usually rely on capillary barrier effects at the interface of the cover layers. These capillary barrier effects appear when a fine-grained material layer overlies a coarse-grained material (e.g. Morel-Seytoux 1992; Shackelford et al. 1994; Stormont 1997; Stormont and Anderson 1999).

The contrast in hydraulic properties between the two materials with opposing textures restricts water flow at the interface. The lower unsaturated hydraulic conductivity, k_u, of the drained coarser-grained material contributes to this effect by limiting downward flow from the fine-grained material, thus favoring water accumulation through capillary forces in the overlying layer (e.g. Akindunni et al. 1991; Bussière et al. 2003; Nicholson et al. 1989). The capillary barrier effects allow water retention in the fine-grained material during the wet periods and its release by evaporation (or evapotranspiration) during the dry periods (Fig. 1). This complex transient hydrogeological behavior is influenced by several factors, such as: the thickness of the water retention layer, the hydrogeological properties (including the hydraulic conductivity and the water retention curve) of the unsaturated materials, the climatic conditions (average and extreme), and sometimes the system inclination (e.g. Aubertin et al. 2009; Khire et al. 2000). Recently, SR covers were designed at Kidston Gold Mines (Australia) and at Barrick Goldstrike Mines (Nevada, US) to control acid rock drainage (ARD) generation from sulfide mine tailings (Williams et al. 2006; Zhan et al. 2001, 2006).

77 % of global phosphate rock reserves are geographically concentrated in Morocco (Cooper et al. 2011). The present study evaluated the possibility of using a SR cover constructed using phosphate waste rock to help control ARD from mine tailings at the abandoned Kettara pyrrhotite ore mine (31° 52′15′′N–8° 10′31′′W), which was exploited by the SYPEK Corporation from 1964 to 1981 (Hakkou et al. 2008a, b). The Kettara mine site, which contains coarse- and fine-grained tailings, is located approximately 35 km north-northwest of Marrakech (Fig. 2) (e.g. Lghoul et al. 2012). This mine site is one of several abandoned mine sites in Morocco that produces ARD that contaminates surface and groundwater (e.g. El Khalil et al. 2008; Sanaa et al. 2011). More information on water contamination at the Kettara site can be found in Hakkou et al. (2008a, b).

The eventual design of a SR cover for the Kettara mine tailings requires adequate cover materials to act as capillary break and store-and-release layers. A recent study (Hakkou et al. 2009) suggested that the Kettara coarse-grained tailings and phosphate limestone wastes from the Ganntour sedimentary basin (Fig. 2—Recette VI) could potentially be used as SR cover components. The first part of this paper summarizes the characterization of the phosphate limestone wastes and coarse Kettara tailings, and describes the design of the field instrumented columns. The second section presents the hydrogeological behavior of the tested columns under natural semiarid climatic conditions. The third segment addresses the behavior of the tested SR covers under extreme precipitation conditions, simulated by adding water to the columns at the start and end of the test period at a rate of up to 155 mm/day. Finally, the performance of the SR cover under simulated extreme precipitation and the difference between laboratory and field water retention curves are discussed.

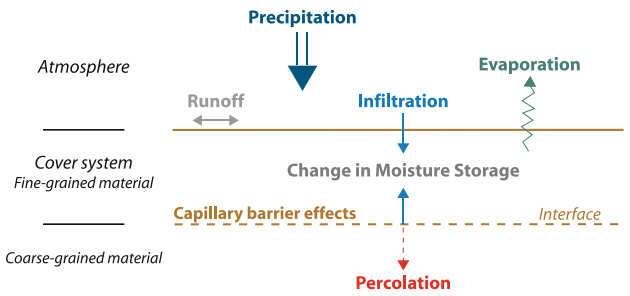

Fig. 1 Schematic representation of store-and-release cover in 1D (*infiltration* subtracting runoff from precipitation; *percolation* deep infiltration)

Materials and Methods

Main Characterization Methods

The phosphate limestone wastes from the "Recette VI" mine site of the Ganntour sedimentary phosphate deposits (Fig. 1) were initially screened in situ to recover the size fraction less than 1 mm. This relatively fine-grained material and the coarse tailings from Kettara were characterized for their chemical and physical properties.

Solids were digested in HNO_3, Br_2, HCl, and HF and the resulting solution was analyzed for elemental chemical composition by inductively coupled plasma-atomic emission spectrometry (ICP-AES) (Perkin Elmer OPTIMA 3100 RL; relative precision of 5 %). Total carbon (TC) was measured under an oxygen atmosphere with an ELTRA PC-controlled CS2000 carbon sulfur determinator.

The particle size distribution was determined using a Malvern Mastersizer laser particle size analyzer for the phosphate limestone wastes and by sieving for the coarse tailings (ASTM D 6913-04 2009; Merkus 2009). The specific gravity was estimated with a Micromeritics Accupyc 1,330 helium gas pycnometer. Standard tests for liquid limit, plastic limit, and plasticity index of materials were performed on the phosphate limestone wastes using the methods described in ASTM D 4318-10 (2010). The saturated hydraulic conductivity (k_{sat}) was also measured for this material using a rigid wall permeameter with the falling-head method (adapted from ASTM D 5856-95 2002). The saturated hydraulic conductivity and the water retention curve of the coarse-grained tailings were estimated using two predictive models: the modified Kozeny-Carman model (Mbonimpa et al. 2002) and the modified Kovács model (Aubertin et al. 2003), respectively. The precision needed in this study for this material justified this approach.

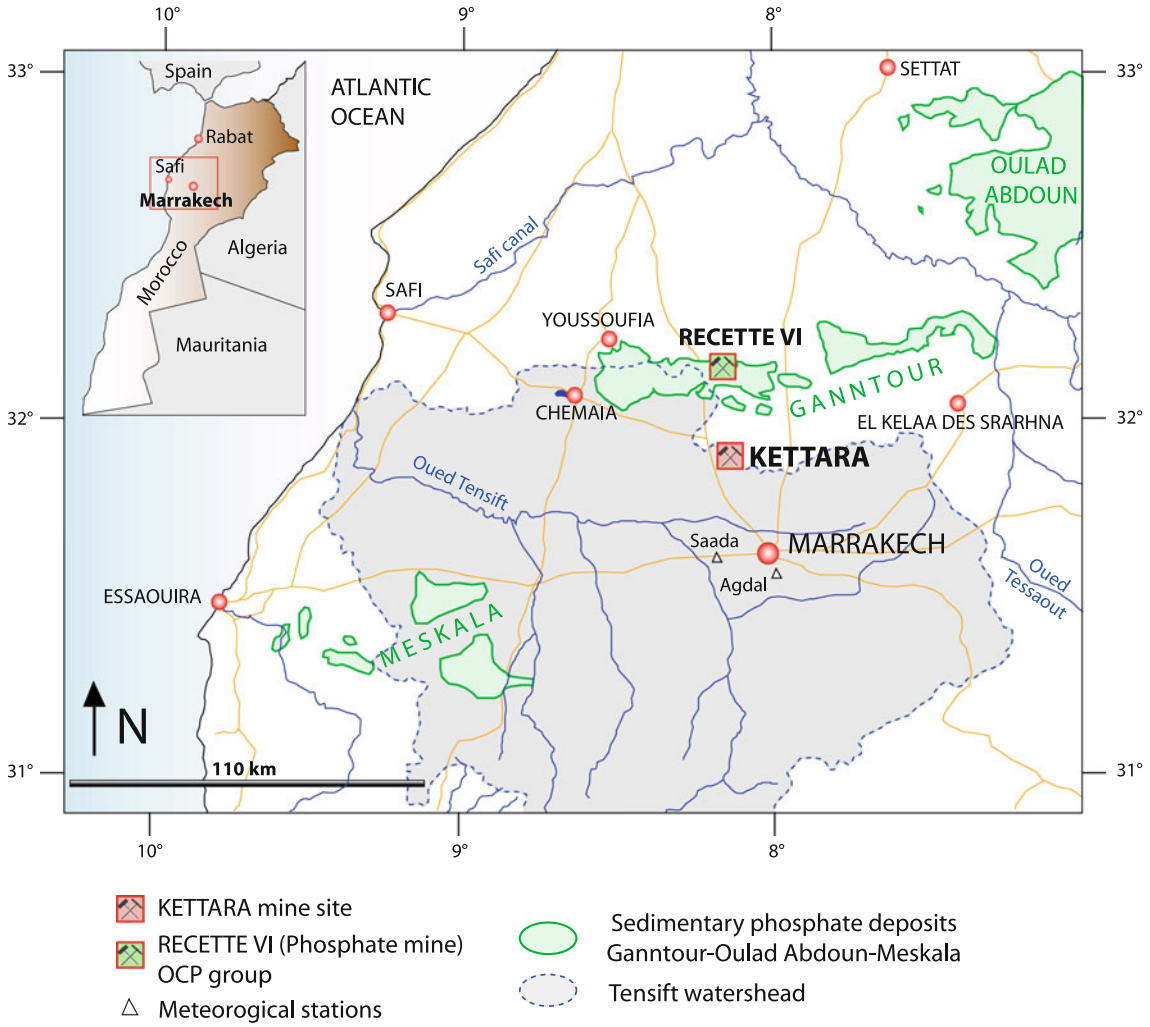

Fig. 2 Location map

The water retention curve (WRC) of the phosphate limestone wastes was obtained from different tests conducted on reconstituted samples having similar porosities. The WRC, which relates the volumetric water content θ (cm^3/cm^3) to the negative pore water pressure ψ (or matric suction—kPa) (e.g. Fredlund and Rahardjo 1993), describes the ability of a given material to store water at different suctions. For suction values between 0 and 1,000 kPa, the WRC was obtained in a Tempe Cell (or pressure chamber), as proposed in ASTM D6836-02 (2008). For higher suction values, saturated salt solutions were used to control the relative humidity in a closed chamber. The thermodynamic relationship between relative humidity and temperature (Eq. 1), was used to evaluate the suction applied (e.g. Fredlund and Rahardjo 1993).

$$\psi = \frac{\rho_w.R.T}{\omega_w}\ln(RH)_T \quad (1)$$

where ψ matric suction [MPa], R universal gas constant [$J.(mol.K)^{-1}$], T absolute temperature [°K], ω_w molecular mass of water vapor [$g.mol^{-1}$], ρ_w density of water [$kg.m^{-3}$], and RH relative humidity.

The matric suction (ψ) generated in the chamber is a function of the saturated salt solution used. Material samples were kept in a closed temperature-controlled chamber (25 °C) under different suctions for 3 months to reach equilibrium. In this study, the relative humidity, or the matric suction, was controlled by solutions made of potassium sulphate (3.8 MPa), sodium chloride (39.1 MPa), magnesium nitrate (87.7 MPa), magnesium chloride (153.5 MPa), and potassium hydroxide (343.7 MPa) (e.g. Greenspan 1977). The weight of each sample, after reaching equilibrium, gives the volumetric water content of the tested materials (phosphate limestone wastes in this case).

Characteristics of the Fine-grained and Coarse-grained Materials

The chemical and mineralogical composition of the fine-grained phosphate limestone wastes was presented by

Table 1 Chemical composition of the phosphate limestone wastes

SiO_2	Al_2O_3	Fe_2O_3	CaO	MgO	Na_2O	K_2O	TiO_2	P_2O_5	F	S	C
Major elements (wt%)											
11.6	0.89	0.38	43.0	3.28	0.46	0.12	0.07	16.9	1.73	0.30	5.20

As	Ba	Be	Cd	Cl	Cr	Cu	Mn	Ni	Pb	Sr	U	V	Y	Zn
Trace elements (ppm)														
8	79.2	0.82	33	108	137	31.8	31.8	34	13	769	88	56	97.8	195

Table 2 Basic properties of the fine-grained and coarse-grained materials

Parameter	Phosphate limestone wastes	Kettara coarse tailings
Specific gravity	2.85	2.90
d_{60} (mm)	7.71×10^{-02}	9.86
d_{30} (mm)	9.09×10^{-03}	5.70
d_{10} (mm)	9.73×10^{-04}	2.84
Coefficient of uniformity	79.24	3.47
Coefficient of curvature	1.10	1.16
Fines content (<80 μm) (%)	55	1
w_L(%)	26.4	–
w_p (%)	25.6	–
PI (%)	0.8	–
Classification (USCS)	Sandy silt	Poorly graded gravel with sand

Hakkou et al. (2009). Table 1 summarizes chemical analysis results that show high contents of CaO (43.0 wt%), P_2O_5 (16.9 wt%), SiO_2 (11.6 wt%), MgO (3.23 wt%), C (5.20 wt%), and potential contaminants, such as F (1.73 wt%), Cr (137 ppm), and Zn (195 ppm). However, Hakkou et al. (2009) showed through kinetic tests that there is no significant contaminant generation from the phosphate limestone wastes. The chemical analysis (Table 1) confirms the mineral composition presented previously by Hakkou et al. (2009) with four main phases: calcite (25–45 %), fluorapatite (25–45 %), dolomite (20–30 %), and quartz (3–10 %).

According to Hakkou et al. (2008a), the coarse-grained Kettara tailings contains between 1.6 and 3.7 wt% total sulfur. Iron, associated with pyrrhotite, pyrite, and iron oxides, is found in large quantities (17.4–22 wt%) than other metals. Significant concentrations of Cu (1,110-2,660 ppm) were also detected, along with lower amounts of Zn (240–500 ppm), Cr (240-330 ppm), Pb (10–80 ppm), Co (30–70 ppm), As (0–70 ppm), Cd (30 ppm), and Ni (40–90 ppm).

The main physical characteristics of the fine- and coarse-grained materials are given in Table 2. The specific gravity (G_s) and the percentage of fines (<80 μm) of the phosphate limestone wastes were respectively estimated at 2.85 and 55 %. The liquid limit is less than 50 % and the plasticity index was estimated to be 0.8. According to the United Soil Classification System (USCS), the material is a non-plastic sandy silt (e.g. McCarthy 2007). The k_{sat} value at a porosity (n) of 0.43 is 5.7×10^{-6} cm/s. The G_s value of the Kettara coarse-grained tailings is 2.90 while the k_{sat} value, estimated with the modified Kozeny-Carman equation, is 1 cm/s (Mbonimpa et al. 2002).The main hydraulic properties for this material, classified as poorly graded gravel with sand, were mainly obtained from predictive models.

Figure 3a shows the experimental drying WRC of the phosphate limestone wastes fitted with the van Genuchten equation (1980; see the parameters of the fitted equation in Fig. 3a) and the drying WRC of the Kettara coarse tailings. The latter was predicted from basic geotechnical properties (Table 2), such as effective grain size diameters (D_{10}; D_{60}) and the coefficient of uniformity (C_U), at a porosity (n) of 0.33. The permeability function that represents the relationships between the hydraulic conductivity and matric suction was obtained from the WRC and the k_{sat} values using the van Genuchten–Mualem model (Van Genuchten 1980). Figure 3b shows the permeability functions of the fine-grained and coarse-grained materials. As is normal in SR cover design (e.g. O'Kane et al. 2000; Scanlon et al. 2005; Wels et al. 2002; Williams et al. 2006; Zhan et al. 2006), the hysteresis effects of the water retention curve (e.g. Maqsoud et al. 2012) and permeability function were not determined in

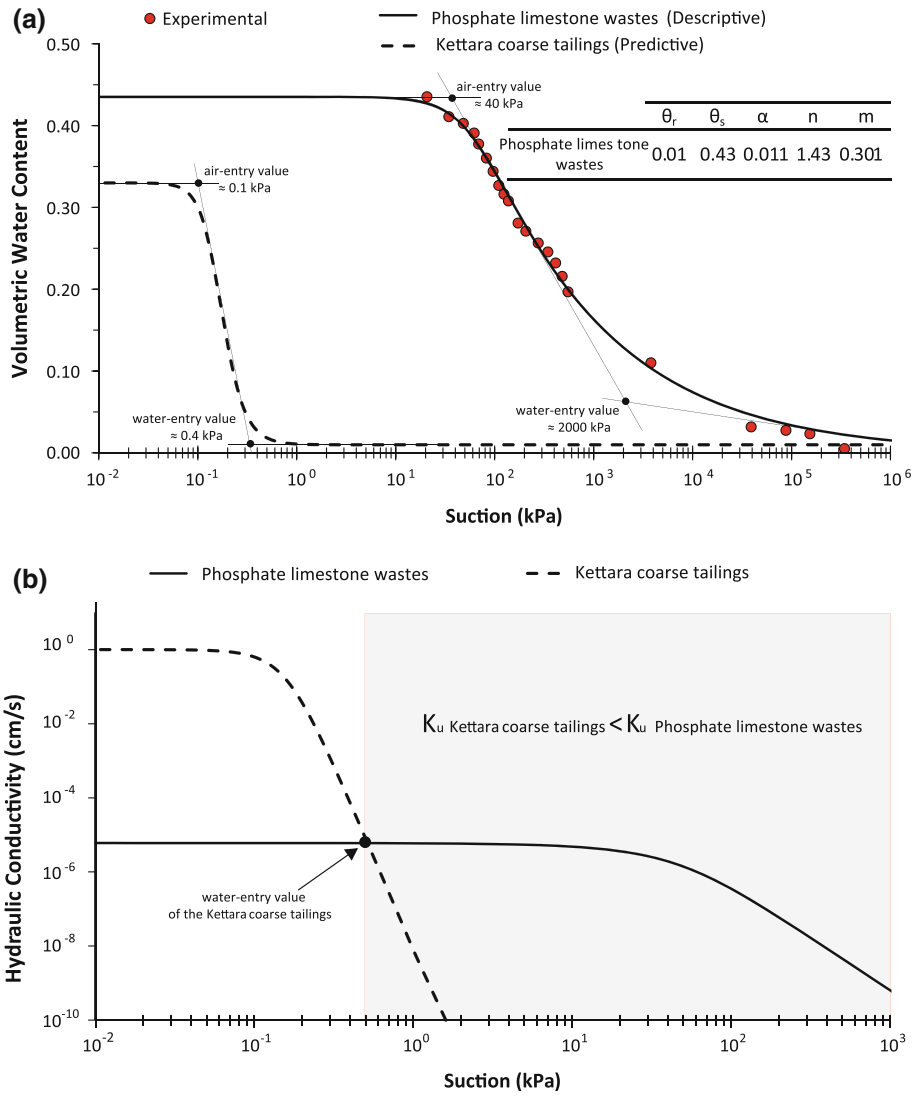

Fig. 3 WRCs (**a**) and permeability functions (**b**) of the fine- and coarse-grained materials

the laboratory. However, hysteresis effects will be discussed further in the paper, using field data.

The unsaturated properties of the two tested materials (Fig. 3) show the contrast in hydraulic properties that is required to create capillary barrier effects. More specifically, the air entry value (pressure at which the material starts to drain—ψ_a) of the fine-grained phosphate limestone wastes is $\sim$40 kPa ($\alpha = 0.011$ kPa^{-1}), while the air-entry value of the coarse-grained Kettara tailings is estimated as close to 0.1 kPa. Hence, the water-entry value (ψ_w—pressure at which the water starts to enter) of the coarse-grained material ($\approx$0.4 kPa) is substantially less than the ψ_a value (40 kPa) of the fine-grained material (Fig. 3a). These values were evaluated using the usual graphical construction procedure (e.g. Chin et al. 2010). In addition, the hydraulic conductivity of the coarse-grained material (Fig. 3b) was less than the hydraulic conductivity of the fine-grained material at suction values close to the ψ_w value. In unsaturated conditions, as long as the water-entry value is not reached, the decrease of the hydraulic conductivity profile should guarantee the presence of capillary barrier effects at the interface between the two materials (Fig. 1) and enhance the storage of water in the fine-grained layer during wet periods (e.g. Khire et al. 1999).

Column Design and Instrumentation

Instrumented columns were designed to assess the store-and-release capacity and the effectiveness of the phosphate limestone waste water-retention layer to limit water infiltration into the underlying mine tailings. These columns are large (60 cm diameter) cylindrical containers manufactured from metallic barrels (Fig. 4) and were filled with reconstituted material and exposed to field climatic conditions to determine water storage and actual evaporation of the cover system at the local scale. The volume and the quality of the collected leachate can be measured at the cylinder bottom (if there is water percolation). The two

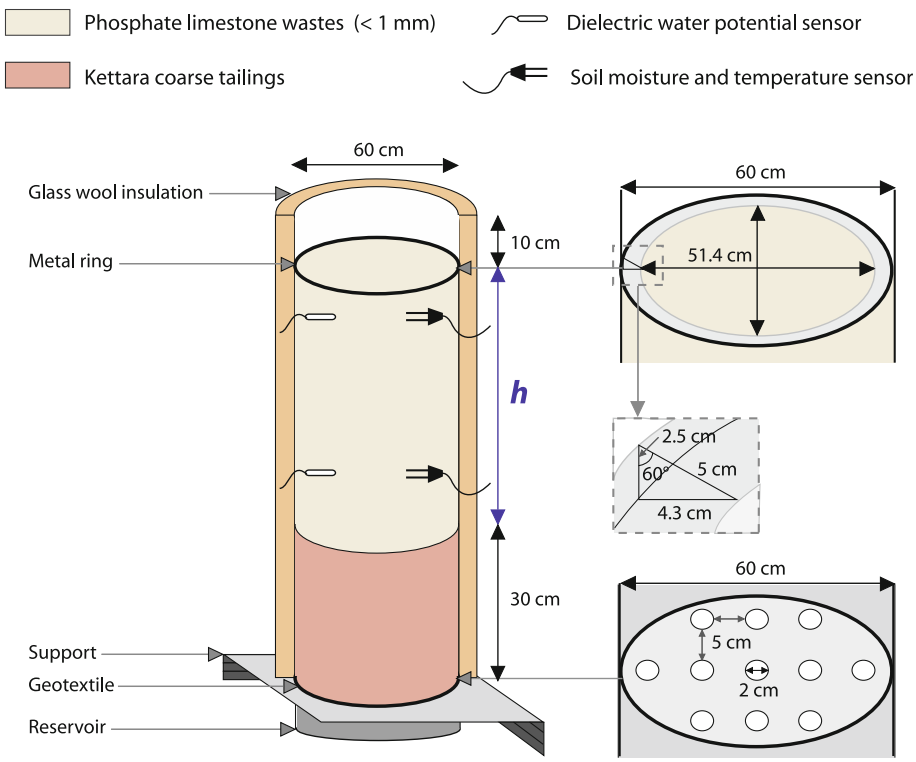

Fig. 4 Scheme corresponding to the column design and monitoring system

columns simulate a SR cover that includes 50 cm (column 1) and 100 cm (column 2) thick layers of phosphate limestone wastes, respectively. The phosphate limestone wastes were homogenized and compacted in successive layers of about 10 cm; 30 cm of Kettara coarse tailings were installed under the phosphate limestone wastes to act as a capillary barrier layer. A metallic ring was installed at the top of each column to avoid circumferential preferential flow (Fig. 4). All columns were protected by internal anti-corrosive paint and external glass wool insulation. Circular holes were drilled at the bottom of the columns to collect the eventual leachate.

The performance of the SR cover and the evaporation assessment were studied by monitoring different parameters of the water balance equation:

$$E = P + Irr - R_o - P_r - \Delta S \quad (2)$$

Actual evaporation (E) is indirectly estimated by subtracting runoff (R_0 nil in a column experiment), percolation (P_r), change in the water storage (ΔS) from precipitation (P), and irrigation (Irr). Climatic data, such as rainfall, solar radiation, relative humidity, and wind speed and direction were obtained from meteorological stations near Marrakech (Fig. 1). Changes in ΔS were monitored using soil moisture ECH_2O sensors (EC-TM) and, indirectly, by suction sensors (MPS-1). It is important to recall that this approach to estimate ΔS has a non-negligible margin of errors (for more information, see Benson et al. 2001, Khire et al. 1999).

The moisture sensors measure the volumetric water content of the soil by measuring its dielectric permittivity while the MPS-1 sensor measures the dielectric permittivity of porous ceramic disks that can be related to the suction into the surrounding soils (Decagon 2007, 2009). EC-TM sensors (which also measure soil temperature) were installed beside the suction sensors (MPS-1) in the center of each column (Fig. 4). Hence, readings of volumetric water contents (θ) can be related to measurements of matric suction (ψ) and in situ WRCs can be derived from these values. For the first column, sensors were installed at 10 and 40 cm depth and for the second column at 25 and 75 cm depth (Fig. 4). A polynomial material-specific calibration curve was determined to obtain more precise volumetric water content measurements (see Bossé 2013 for more details); the calibration curve can be applied to all soil moisture sensors. The annual soil temperature was not considered in the calibration process. According to Kizito et al. (2008), for a temperature change of 10 °C, measurements of volumetric water contents are affected by approximately 0.02 (cm^3/cm^3). Hence, temperature effects are not negligible and could influence measured time-trends. The suction sensors (MPS-1) measure the matric suction between 10 and 500 kPa without user maintenance, and a material-specific calibration curve (Decagon 2009). Malazian et al. (2011) have shown a maximum difference of 10 kPa between measurements with calibrated MPS-1 sensors and tensiometers, for suction values between 10 and 60 kPa. In addition, measurements during the present

study suggest that measurements are less reliable for suctions values higher than 200 kPa (see Bossé 2013 for details). The monitoring period of the columns started in May 2010 and was maintained for a period of one and a half years (until January 2012).

Results

Climatic Conditions

The climate of the Kettara mine and the monitoring site in Marrakech is semiarid (aridity index: 0.21). Typically, semiarid climates are dominated by wet and dry season succession. The meteorological data of the Agdal station (Fig. 1) were considered representative of the column conditions.

Figure 5a shows average daily air temperatures measured at the Agdal meteorological station. For the studied period, the lowest average daily air temperature (5.9 °C) occurred in February (2011) and the highest (35.5 °C) in August (2010). The average annual air temperature (2011) was about 18.5 °C. Figure 5b and c respectively present daily potential evapotranspiration (PET) assessed from climatic data of the Agdal meteorological station (solar radiation, relative humidity, temperature, and wind speed) using the Penman–Monteith method (Allen et al. 1998) and average daily rainfalls. During the monitoring period, the cumulative rainfall and the PET were respectively evaluated at 334 and 2,178 mm. The largest rainfall occurs normally from the end of fall to spring when temperatures are at their lowest (Fig. 5). With 10 % of the total annual precipitation, June, July and August are the driest months; low rainfall, warm temperatures, and high potential evapotranspiration characterize this dry season.

Volumetric Water Contents and Suction Measurements

Volumetric water content and suction time-series were measured within the fine-grained material (phosphate limestone wastes) at depths of 10 and 40 cm for the first column (Figs. 6a, 7a) and 25 and 75 cm for the second column (Figs. 6b, 7b); the average daily rainfall is also presented in these figures. The volumetric water content peaks, initially and at the end of the test, are due to simulated extreme events that will be discussed later.

After the initial peak, soil moisture sensors indicated a preliminary decrease of volumetric water contents in the soil profile due to the release of water through evaporation. The volumetric water content measurements decreased from approximately 0.30–0.07 at the top of both columns during the dry seasons (from June to Sept. 2010 and 2011). Many fluctuations, corresponding to a succession of wetting and drying cycles, were observed during the testing period with greater magnitudes during the wet seasons. Between Nov. 2010 and June 2011, the volumetric water content (measured at 10 cm) fluctuated significantly. The rate and fluctuation magnitude of volumetric water contents were more pronounced at 10 cm than at the 40 cm depth. Indeed, at 40 cm, a gradual increase of the volumetric water content to values less than 0.17 is observed from March (2011) to July (2011), followed by a gradual decrease. For the second column, a gradual increase in volumetric water content occurred at the 25 cm depth between March and June (2011), with a maximum volumetric water content of approximately 0.17. A final increase was detected between Nov. 2011 and the end of the monitoring period due to the second wet season. At a depth of 75 cm, the last simulated extreme event was not detected, as volumetric water contents stayed close to the residual water content (0.05) of the fine-grained material for the entire testing period.

Figure 7a and b show matric suction measurements for columns 1 and 2, respectively. The suction sensors indicate a preliminary increase of the suction in the soil profile due to the release of water by evaporation. Thus, for the first column and after the initial wetting, the suction increases during the dry seasons for both depths (10 and 40 cm). After a dry season, final suctions are higher than 200 kPa. In the case of the 10 cm suction sensor, many fluctuations were observed, particularly during the wet season. As seen for the volumetric water contents, the suction value and fluctuation magnitudes were greater at 10 cm than at 40 cm. The matric suction measurements of the top sensor varied between 50 and >200 kPa over a relatively short period of time. At 40 cm, a gradual suction decrease (typically from <200 to 50 kPa) was observed from April 2011 to June 2011, followed by a gradual increase. For the second column, the two sensors located at 25 and 75 cm depths exhibited a similar behavior, except during wet seasons when the 25 cm sensor fluctuated, but the 75 cm sensor did not. The 75 cm sensor seemed to have a cyclic behavior between wet and dry seasons with suction values >200 kPa (which is the upper limit of precision for the sensor MPS-1).

To summarize the hydrogeological behavior of the two tested columns, volumetric water content and suction time-series showed a seasonal pattern of water storage and water release to the atmosphere by evaporation. After each dry season, the volumetric water content decreased to values between 0.05 and 0.10, while the volumetric water content (θ) after the wet season increased to values close to full saturation (0.40) near the surface (10 cm). Deeper, θ values were more constant with a maximum θ usually less than 0.17. The suction measurements were relatively well correlated to the volumetric water content with minimum ψ values measured close to the surface

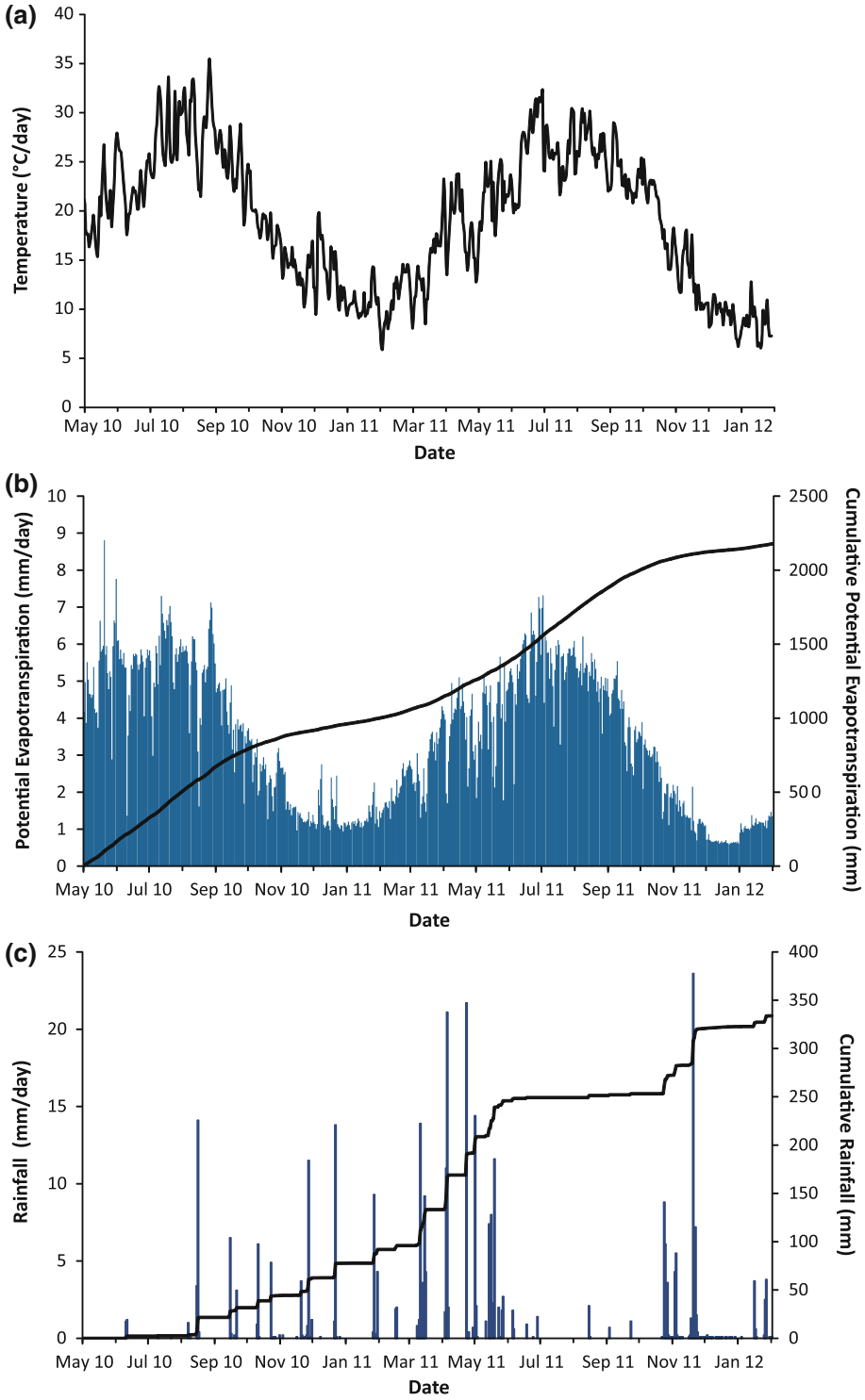

Fig. 5 Average daily air temperatures (**a**), potential evapotranspiration (**b**), and rainfall (**c**), between May 2010 and Jan. 2012

(10 cm), where the highest θ values were observed. Moreover, the highest ψ values (> 200 kPa) were measured when the θ measurements were close to the residual value (observed during dry seasons). The suction gradient was clearly upward during the dry seasons with a greater suction close to the surface.

Water Balance and Actual Evaporation Assessment

The store-and-release capacity for the two columns was estimated using the water balance equation (Eq. 2) and the actual evaporation was calculated, as discussed above. The water storage in the phosphate limestone wastes was

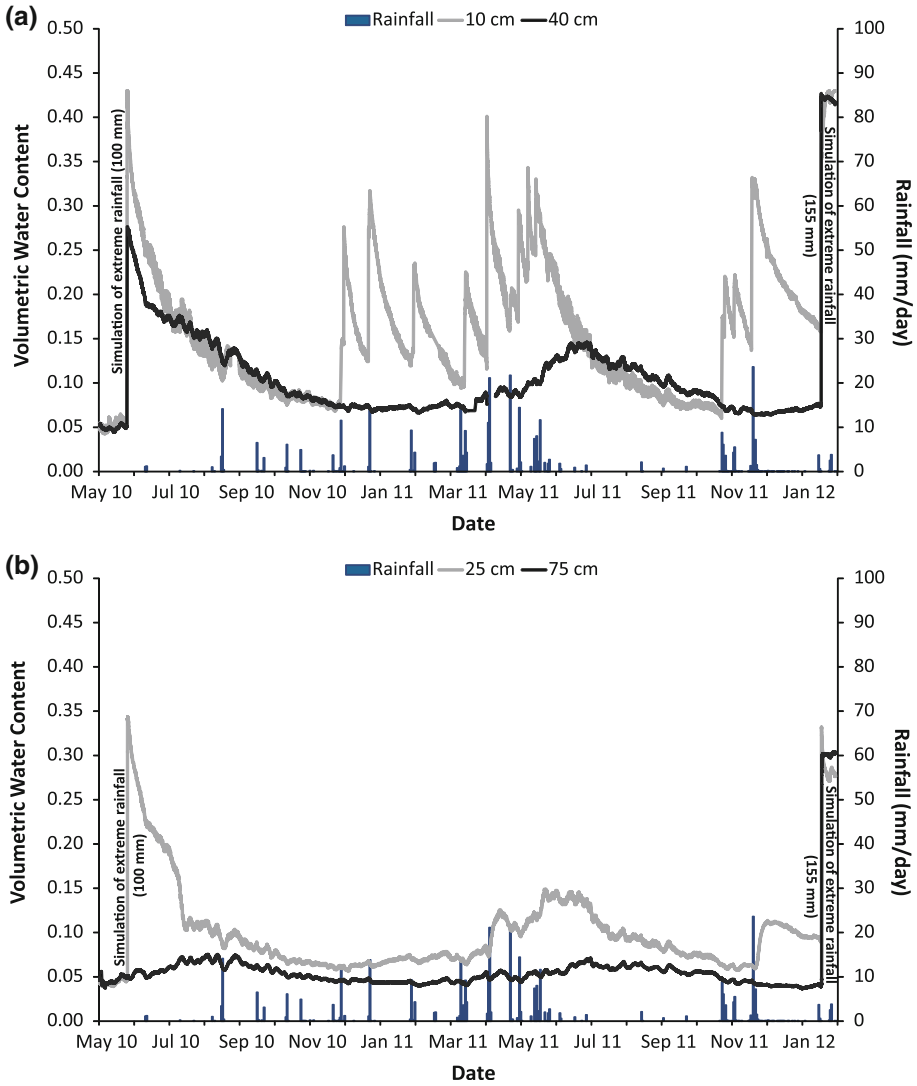

Fig. 6 Time-trends of volumetric water content at depths of 10 and 40 cm (**a**), and 25 and 75 cm (**b**), between May 2010 and Jan. 2012

calculated by integrating the volumetric water content profiles during the monitoring period (e.g. Albright et al. 2004; Benson et al. 2001; McGuire et al. 2009; Stormont and Morris 1998; Waugh et al. 2008; Wels et al. 2002). Figure 8a and b show the daily water storage time-series for the columns, which included 50 and 100 cm of phosphate limestone wastes, respectively. These time-series correlate with the average daily rainfall; the water storage decreases during dry season and shows several fluctuations during the wet season. For the tested monitoring period, excluding the two simulated extreme events (discussed later), both covers show water storage between 5 and 36 mm/day (Fig. 8a, b). The maximum value of the daily water storage was 36 mm/day and occurred in May 2011. In addition, more significant variations and usually higher water storage values (for a given date) were observed for the 50 cm thick cover.

The other components of the water balance equation allowed assessment of the actual evaporation for the two columns. The top surface of the bare material was flat and, except for the last extreme event simulation, no leachate was collected. Hence, runoff and drainage can be neglected (Eq. 2). Table 3 shows the monthly water balance during 2011, while Fig. 8a and b summarize the daily water balance data for each column. The two figures show a similar trend for the two columns with a rate of evaporation comparable to the rate of rainfall. Depending on the climatic conditions and more particularly on the rainfall distribution, specific periods can be identified. After the initial extreme event of 100 mm (end of May 2010), a rapid evaporation event is observed during the first summer. Then the evaporation rate decreases due to rainfall during the wet season. Significant rainfall events induce an increase in cumulative rainfall and water storage between March and May 2011, just before the second dry season. Finally, cumulative rainfall increases again in November 2011, while the evaporation rate decreases.

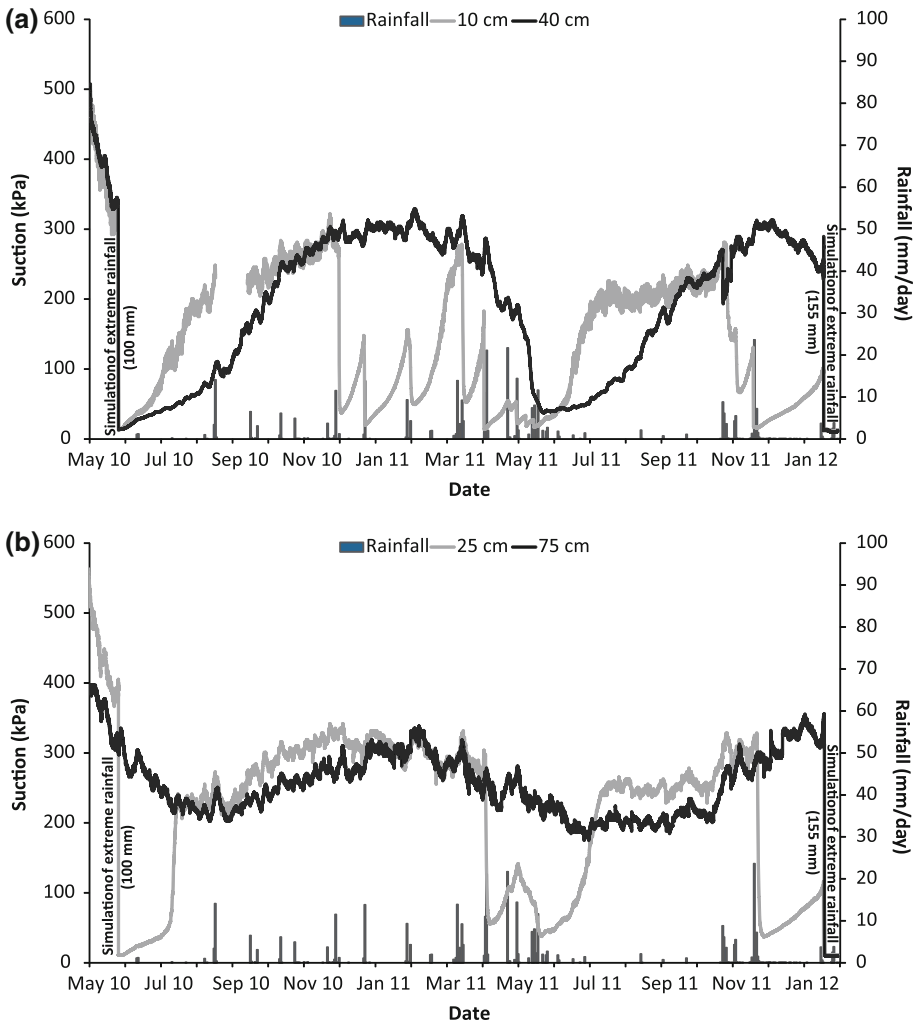

Fig. 7 Time-trends of matric suction at depths of 10 and 40 cm (**a**), and 25 and 75 cm (**b**), between May 2010 and Jan. 2012

As shown in Table 3, the physical process of evaporation occurs mainly during the spring and at the beginning of the summer seasons. For example, if we exclude the influence of the extreme simulated precipitation events, the most important rate of evaporation (between 45 and 55 mm) happens during April. From June to Sept. 2011, with low total rainfall (8.8 mm), high potential evapotranspiration (741.5 mm), and significant water storage (84.2 mm for the 50 cm thick cover and 57.3 mm for the 100 cm thick cover), the actual evaporation from the fine-grained material is lower than 15 % of the total annual rainfall (29.2 mm for the 50 cm thick cover and 35.7 mm for 100 cm thick cover). For the two columns, net infiltration is estimated at approximately 246.5 mm and the actual evaporation is estimated at 245.7 and 231.5 mm, respectively, for the 50 and 100 cm cover (Table 3). Hence, in 2011, for columns 1 and 2, 99.7 and 93.9 % of the rainfalls were respectively released to the atmosphere by evaporation. For the second column, estimated values could be underestimated due to the location of sensors (25 cm deep), which are relatively far from the effective portion of the SR cover (the first 10 cm) (Benson et al. 2001).

Discussion

SR Cover Behavior for Extreme Conditions

As discussed previously, two extreme events were simulated by adding a known volume of water over a period of 24 h. The behavior of SR covers when exposed to these extreme conditions is important since the designed SR cover must be efficient for both average expected values and extreme events (i.e. extreme precipitation in this case). Extreme events are usually based on return periods with a small occurrence probability (e.g. Zhan et al. 2001). The first event simulated a precipitation of 100 mm in 24 h; the event was simulated at the start of the test period at the end of May 2010 (Fig. 9a). The second event of about 155 mm

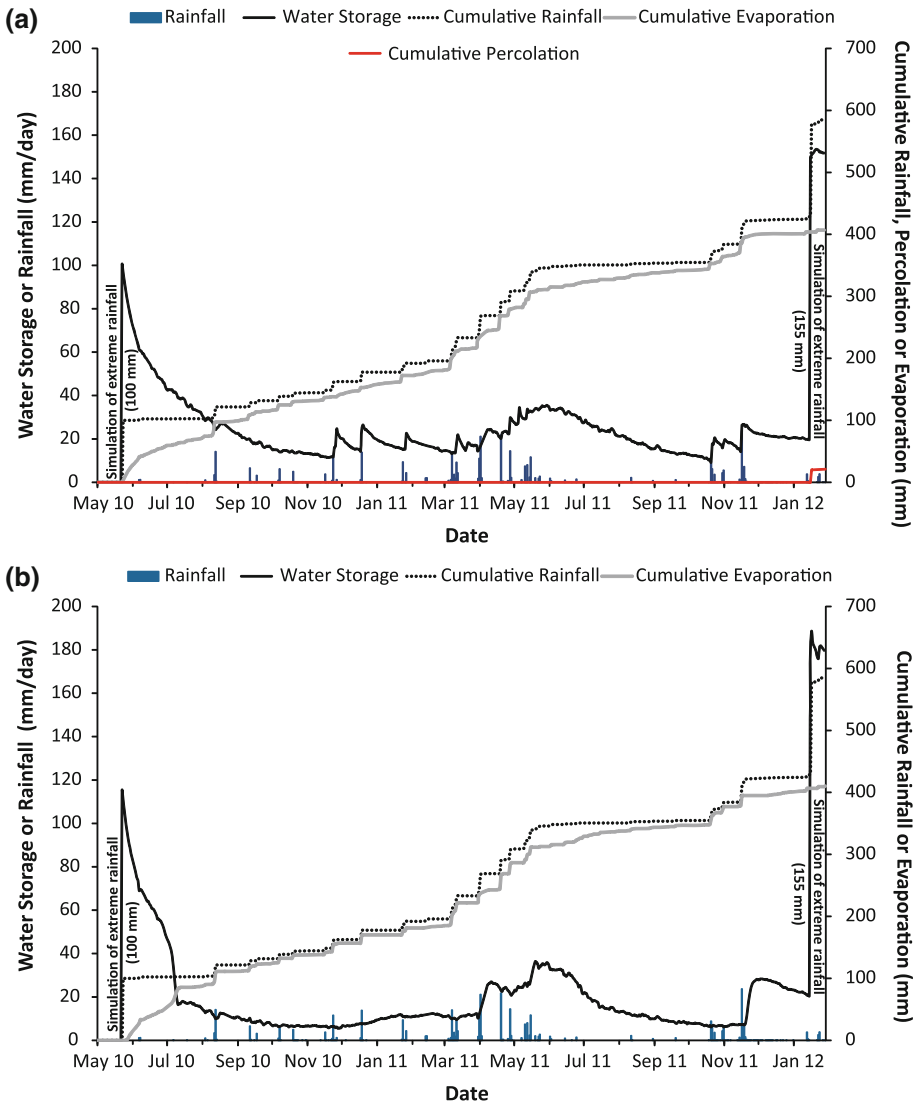

Fig. 8 Daily water balance for the columns with 50 (**a**) and 100 (**b**) cm of phosphate limestone wastes

of rain in 24 h was simulated at the end of the monitoring period (Jan. 2012) (Fig. 9b). These extreme events were selected to represent long- return period rainfall events calculated using normal methods, such as the Hershfield (1965) statistical method and the Gumbel (1958) distribution. Daily rainfall distribution data between 1999 and 2011 at the Saada and Agdal meteorological stations (Fig. 1) were used to estimate these events. The Hershfield method (1965) was used to estimate the probable maximum precipitation (PMP) from measured rainfall, the mean and standard deviation of the series, and a frequency factor between 5 and 20 (Koutsoyiannis 1999). PMP is defined as "theoretically the greatest depth of precipitation for a given duration that is physically possible over a given size storm area at a particular geographical location at a certain time of the year" (WMO 1986). Using maximum daily rainfall values, between 1999 and 2011, and with a frequency factor of 18.5, the 24 h PMP was estimated at 155 mm. Koutsoyiannis (1999) showed that the PMP estimated by the Hershfield method has a return period of approximately 60,000 years. According to Papalexiou and Koutsoyiannis (2006) a probabilistic approach, such as the Gumbel distribution (1958), is another reasonable method to identify extreme events. For a return period of 60,000 years, the Gumbel distribution suggests a maximum daily rainfall of approximately 80 mm. Knowing that Gumbel distributions usually underestimate maximum daily rainfall (e.g. Koutsoyiannis 1999, 2003), it was decided to use 100 mm as the other value for the tested extreme events.

Figure 9 shows volumetric water content profiles at 10, 25, 40, and 75 cm depths for both columns, before and after the two extreme event simulations. For the 100 mm extreme event (Fig. 9a), a gradual increase of the volumetric water content was observed for both columns. For the column with 100 cm of phosphate limestone wastes, the sensor located at the bottom (75 cm) was not affected by the extreme event

Table 3 Monthly water balance (in mm) for columns containing 50 and 100 cm of phosphate limestone waste rock

Month	Column 1 (50 cm)									Column 2 (100 cm)			
	P	*PET*	*Irr*	R_o	*Net I*	P_r	ΔS	*E*	*S*	P_r	ΔS	*E*	*S*
Jan-11	14.3	40.1	0	0	14.3	0	0.30	14.0	22.5	0	2.70	11.6	11.1
Feb-11	3.90	56.3	0	0	3.90	0	−7.70	11.6	14.8	0	0.50	3.40	11.7
Mar-11	37.3	87.2	0	0	37.3	0	2.30	35.0	17.1	0	0.30	37.0	12.0
Apr-11	59.0	114.4	0	0	59.0	0	5.30	53.7	22.4	0	11.0	48.0	23.0
May-11	53.7	123.6	0	0	53.7	0	12.6	41.1	35.0	0	12.3	41.4	35.3
Jun-11	4.80	165.0	0	0	4.80	0	−5.70	10.5	29.3	0	−10.7	15.5	24.5
Jul-11	0.00	173.7	0	0	0.00	0	−5.80	5.8	23.5	0	−10.2	10.2	14.4
Aug-11	2.20	159.3	0	0	2.20	0	−7.40	9.6	16.1	0	−4.30	6.50	10.0
Sep-11	1.80	119.9	0	0	1.80	0	−2.60	4.4	13.4	0	−1.60	3.40	8.40
Oct-11	19.1	80.2	0	0	19.1	0	4.60	14.5	18	0	−1.50	20.6	6.90
Nov-11	48.4	41.8	0	0	48.4	0	5.10	43.3	23.1	0	19.9	28.5	26.8
Dec-11	2.00	20.5	0	0	2.00	0	−0.20	2.20	22.9	0	−3.40	5.40	23.4
2011	246.5	1,182	0	0	246.5	0	0.8	245.7	258.1	0	15	231.5	207.5

P precipitation, *PET* potential evapotranspiration, *Irr* irrigation, R_0 runoff, *Net I* net infiltration, P_r percolation, ΔS water storage change, *E* actual evaporation, *S* water storage at end of the month

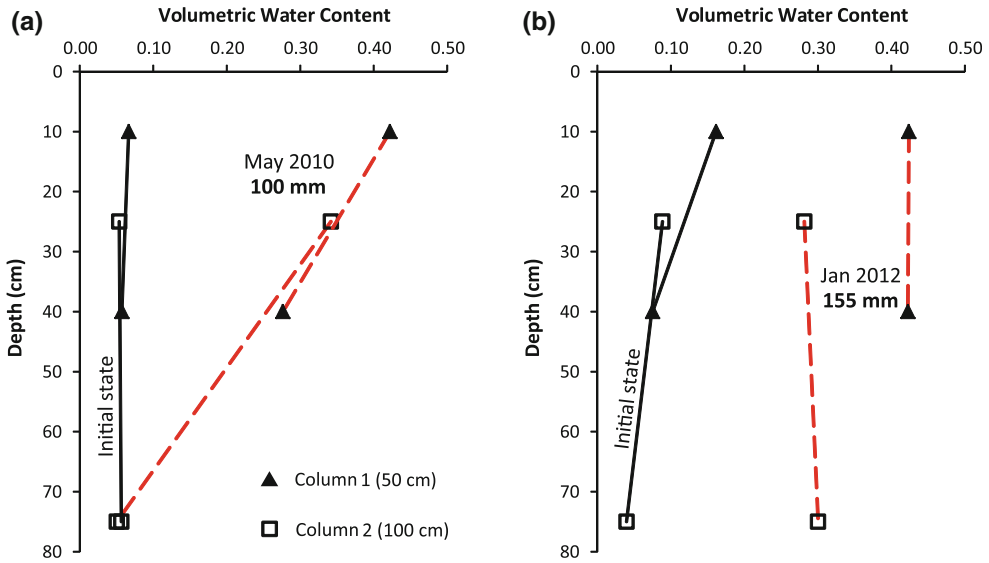

Fig. 9 Measured volumetric water content profile: (**a**) extreme event simulation of 100 mm; (**b**) extreme event simulation of 155 mm

while the one located at the bottom of the 50 cm column (40 cm) showed an increase of the volumetric water content (from 0.05 to 0.28). This means that full saturation (which corresponds to a volumetric water content = porosity (n) = 0.43) was not reached at 40 or 75 cm. The sensors located at the top of both columns were affected with maximum volumetric water content of 0.43 (at 10 cm), and 0.34 (at 25 cm), for the 50 cm and 100 cm columns, respectively. It is important to note that the first extreme event was tested with initially dry conditions.

The hydrogeological behavior of both covers is different when columns were exposed to the 155 mm extreme rainfall event simulation (Fig. 9b); the initial volumetric water content profile of the columns was different than in the first test, with values close to the residual value (instead of being dry). For the 50 cm thick cover, the volumetric water content at both the 10 and 40 cm depths reached the saturation value of 0.43. This means that the cover was saturated, which explains the percolation measured (20 mm) at the bottom of the column (Fig. 8a). When the cover becomes saturated, the capillary barrier effects at the interface between the coarse-grained and the fine-grained layers disappear, which allows downward water flow (Morel-Seytoux 1992). The 100 cm thick cover did not show the same behavior, with volumetric water content values lower than the saturation value (0.43). Indeed, the maximum volumetric water content was approximately 0.30 at both the 25 and 75 cm depths. No percolation was

measured at the bottom of the 100 cm column due to the presence of the capillary barrier effects at the interface.

It is worth mentioning that the collected leachate at the bottom of column 1 had a pH of 3.46, an Eh of 238 mV, and an electrical conductivity of 2.20 mS/cm. These values are typical of ARD. Hence, in the case of an extreme event of 155 mm, a SR cover of 50 cm made of phosphate limestone wastes over the Kettara coarse tailings did not provide control of ARD.

Comparison Between Measurements and the WRC

Simultaneous measurements of volumetric water content (θ) and suction (ψ) at 10, 25, and 40 cm depths (Figs. 6, 7) were compared to the laboratory water retention curve of the phosphate limestone wastes, obtained during the drainage of a fully saturated material (designated as the main drying curve: MDC) (Fig. 3a). For suction values less than 200 kPa (values for which the MPS-1 sensor is reliable), Fig. 10 shows that most of the θ-ψ points are below the MDC of the phosphate limestone wastes. Scanning curves typical of hysteresis effects are also observed in Fig. 10. These hysteresis effects indicate that the WRC of the tested material is not unique and that the θ-ψ relationship depends on the wetting or drying paths that apply in the field (Davis et al. 2009; Haines 1930; Haverkamp et al. 2002; Miller and Miller 1956; Mualem and Beriozkin 2009; Poulovassilis 1962). The observed scanning curves appeared mainly in the wet seasons, at the 10 cm depth, after rainfalls of more than 20 mm in 24 h (e.g. April and Nov. 2011; Fig. 5c).

Our measurements were compared with the predicted main wetting curve (MWC) given by the first wetting cycle of a dry material using the modified Kovács model with hysteresis effects (MK_h) (Maqsoud et al. 2012). This model was recently proposed to predict hysteresis effects of water retention curves for granular materials (non-cohesive, low plasticity). The MWC is predicted from basic geotechnical properties such as effective grain size diameters (D_{10}; D_{60}), the coefficient of uniformity (C_U), the void ratio ($e = n/(1-n)$), and the contact angle during the wetting process (β_w). Fig. 10 presents the MWC of the phosphate limestone wastes (Table 2), at a porosity (n) of 0.43 and a contact angle of 70° (to get the best fit to experimental data).

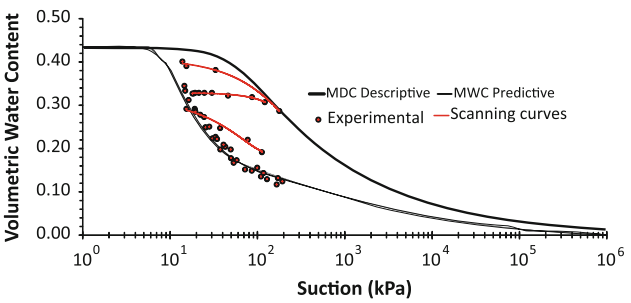

Fig. 10 Hysteresis effects of the water retention curve

To summarize, Fig. 10 shows the MDC and the MWC of the fine-grained phosphate limestone wastes with some selected field data. All measurements are located between the MWC and MDC (usually closer to the MWC) confirming that hysteresis effects are present in the phosphate limestone wastes in the field. This observation is important and means that, especially under semiarid climate conditions, using only the MDC to predict the hydrogeological behavior of the SR cover made of phosphate limestone wastes would not be appropriate and could lead to unrealistic predictions of the soil water storage capacity and, consequently, to an inappropriate cover design.

Other Remarks

These tests, which were performed in a semiarid climate, showed that rainfall was successfully stored in the phosphate limestone wastes and later released to the atmosphere by the two tested SR covers. However, column tests are limited. For example, Benson et al. (2007) and Smesrud et al. (2012) showed that hydrogeological soil properties of SR covers can change over time. This aspect must be investigated further with the tested materials.

Another important factor that could affect SR cover performance is site geometry, since the inclination of a cover system can affect the capacity of the system to control percolation. The infiltration water accumulates above the tilt interface until the suction approaches the water-entry value (or water-entry pressure) of the coarse-grained material (Steenhuis et al. 1991). At this particular location (called the down dip limit by Ross 1990), where the pressure at the interface is greater than the water-entry value of the coarse-grained material, water can move downward into the Kettara tailings, and the cover can no longer control ARD generation effectively. If the SR cover technology is applied on the Kettara site, it will be important to validate that the system would also be effective on the side slopes of the site (e.g. Zhan et al. 2001, 2006).

Finally, a vegetative cover is usually implemented on a SR cover to increase water removal by the biophysical process of transpiration and to control erosion phenomena (e.g. Rock et al. 2012; Smesrud et al. 2012). This influence of vegetative cover must also be integrated into the final design of the cover system.

Conclusions

The assessment of phosphate limestone wastes as a component of SR covers with capillary barrier effects was investigated; in this study, coarse tailings from an existing

abandoned mine site located in Morocco (the Kettara site) was used as the capillary break layer. Two SR covers of 50 and 100 cm of fine-grained phosphate limestone wastes were tested over the capillary break layer in instrumented columns to evaluate the store-and-release capacity and the effectiveness of the water-retention layer to control water percolation. The main observations of this study were:

- Under natural climatic conditions, sensors at depths of 10, 25, and 40 cm were affected by rainfall but no water percolation was collected. In addition, after each dry season, the volumetric water content profile of the fine-grained material returned close to the residual water content. For both SR covers tested, the fine-grained material overlying the coarse-grained material successfully stored and released meteoric waters.
- Sensors at depths of 10, 25, 40, and 75 cm were affected by simulated extreme precipitation events. Additionally, capillary barrier effects broke down at the interface between the coarse- and fine-grained layers after the 155 mm/day rainfall in the column that contained only 50 cm of phosphate limestone wastes, and ARD water percolated through the cover system. For the column that contained 100 cm of phosphate limestone wastes, no water percolation was observed after either the 100 mm/day or the 155 mm/day simulated event.
- Hysteresis effects were observed in the water retention curve of the phosphate limestone wastes in the field.

This study suggests that a suitable thickness of the store-and-release layer is between 50 and 100 cm. This preliminary investigation for the reclamation of the Kettara mine site suggests that nearby phosphate limestone wastes have the appropriate properties to become part of an efficient SR cover to control ARD generation. Nevertheless, some further work is required to refine the design thickness of the store-and-release layer and system inclination. Other tests at a pilot scale directly on the Kettara tailings storage area are recommended before constructing the full scale SR cover (e.g. Albright et al. 2004; Benson et al. 2001; Bussière et al. 2007; Nyhan 2005; Scanlon et al. 2005; Waugh et al. 2008; Wels et al. 2002). Finally, a comparison between transient hydrogeological behavior of the tested SR cover systems and numerical prediction is the next logical step. Integrating the hysteresis effects of the phosphate limestone wastes into the numerical modeling in parallel with the soil/atmosphere interactions is recommended to assess the likely long-term performance of the covers.

Acknowledgments Financial support for this study was provided through the International Research Chairs Initiative, a program funded by the International Development Research Centre (IDRC) and the Canada Research Chairs program. Phosphate limestone wastes were kindly made available by the OCP group (Office Chérifien des Phosphates) and meteorological data were provided by the International Joint Laboratory LMI TREMA and SUDMED project involving the collaboration of CESBIO (Centre d'Etudes Spatiales de la Biosphère, France) the Cadi Ayyad University (Morocco), the Agriculture Office (Office de Mise en Valeur Agricole), and IRD (Institut de Recherche pour le Développement, France). Finally, the authors thank the anonymous reviewers for their constructive comments.

References

Akindunni FF, Gillham RW, Nicholson RV (1991) Numerical simulations to investigate moisture-retention characteristics in the design of oxygen-limiting covers for reactive mine tailings. Can Geotech J 28:446–451

Albright WH, Benson CH, Gee GW, Roesler AC, Abichou T, Apiwantragoon P, Lyles BF, Rock SA (2004) Field water balance of landfill final covers. J Environ Qual 33(6):2317–2332

Albright WH, Benson CH, Waugh WJ (2010) Water balance covers for waste containment. Principles and Practice. ASCE Press, Reston, VA

Allen RG, Pereira LS, Raes D, Smith M (1998) Crop evapotranspiration (guidelines for computing crop water requirements). FAO Irrigation and Drainage Paper 56, http://www.kimberly.uidaho.edu/ref-et/fao56.pdf

ASTM (2002) D 5856-95: Standard test methods for measurement of hydraulic conductivity porous materials using a rigid-wall, compaction-mold permeameter. Annual Book of ASTM Standards Vol 04.08

ASTM (2008) D 6836-02: Standard test methods for determination of the soil water characteristic curve for desorption using a hanging column, pressure extractor, chilled mirror hygrometer, and\or centrifuge. Annual Book of ASTM Standards Vol 04.08

ASTM (2009) D 6913-04: Standard test methods for particle-size distribution (gradation) of soils using sieve analysis. Annual Book of ASTM Standards Vol 04.09

ASTM (2010) D 4318-10: Standard test methods for liquid limit, plastic limit, and plasticity index soils. Annual Book of ASTM Standards Vol 04.08

Aubertin M, Mbonimpa M, Bussière B, Chapuis RP (2003) A model to predict the water retention curve from basic geotechnical properties. Can Geotech J 40:1104–1122

Aubertin M, Cifuentes E, Apithy SA, Bussière B, Molson J, Chapuis RP (2009) Analyses of water diversion along inclined covers with capillary barrier effects. Can Geotech J 46:1146–1164

Barnswell KD, Dwyer DF (2011) Assessing the performance of evapotranspiration covers for municipal solid waste landfills in Northwestern Ohio. J Env Eng ASCE 137(4):301–305

Benson CH, Abichou T, Albright WH, Gee GW, Roesler AC (2001) Field evaluation of alternative earthen final covers. Int J Phytorem 3:1–21

Benson CH, Albright WH, Roesler AC, Abichou T (2002) Evaluation of final cover performance: field data from the alternative cover assessment program (ACAP). Proc, WM'02 Conf, Tucson, AZ, USA, https://www.dri.edu/images/stories/research/programs/acap/acap-publications/8.pdf

Benson CH, Sawangsuriya B, Trzebiatowski B, Albright WH (2007) Post-construction changes in the hydraulic properties of water balance cover soils. J Geotech Geoenv Eng 133(4):349–359

Bossé B (2013) Evaluation du comportement hydrogéologique d'un recouvrement « Store-and-Release » constitué de rejets calcaires phosphatés en climat semi-aride. PhD Diss, UQAT, Rouyn-Noranda, Canada

Bussière B, Aubertin M, Chapuis R (2003) The behaviour of inclined covers used as oxygen barriers. Can Geotech J 40(3):512–535

Bussière B, Aubertin M, Mbonimpa M, Molson JW, Chapuis RP (2007) Field experimental cells to evaluate the hydrogeological behaviour of oxygen barriers made of silty materials. Can Geotech J 44:245–265

Chin KB, Leong EC, Rahardjo H (2010) A simplified method to estimate the soil-water characteristic curve. Can Geotech J 47:1382–1400

Cooper J, Lombardi R, Boardman D, Carliell-Marquet C (2011) The future distribution and production of global phosphate rock reserves. Resour, Conser and Recyc 57:78–86

Daniel DE, Koerner RM (2007) Waste containment facilities: guidance for construction quality assurance and construction quality control of line and cover system, 2nd edn. ASCE Press, Reston, VA

Davis DD, Horton R, Heitman JL, Ren TS (2009) Wettability and hysteresis effects on water sorption in relatively dry soil. Soil Sci Soc Am J 73:1947–1951

Decagon (2007) ECH2O-TE/EC-TM water content, EC and temperature sensors. Operator's manual, Decagon Devices Inc, Pullman WA, USA

Decagon (2009) Dielectric water potential sensor. Operator's manual, version 3, Decagon Devices Inc, Pullman WA, USA

Dwyer SF (2003) Water balance measurements and computer simulations of landfill covers. PhD Diss, Univ of New Mexico, Albuquerque, NM, USA

El Khalil H, El Hamiani O, Bitton G, Ouazzani N, Bourlarbah A (2008) Heavy metal contamination from mining sites in South Morocco: monitoring metal content and toxicity of soil runoff and groundwater. Env Monit Assess 136:147–160

EPA (2011) Fact sheet on evapotranspiration cover systems for waste containment. US Environmental Protection Agency, Washington DC, USA, http://www.epa.gov/tio/download/remed/epa542f11001.pdf

EPA (2012) Evapotranspiration covers. Technology innovation and fields services division. US Environmental Protection Agency, Washington DC, USA, http://www.clu-in.org/products/evap/

Fredlund DG, Rahardjo H (1993) Soil Mechanics for Unsaturated Soils. Wiley, NYC, NY

Gee GW, Benson CH, Albright WH (2006) Comment on "evaluation of evapotranspirative covers for waste containment in arid and semiarid regions in the southwestern USA". Vadose Zone J 5:809–812

Greenspan L (1977) Humidity fixed points of binary saturated aqueous solutions. J Res Nat Bur Stan 81A(1):89–96

Gumbel EJ (1958) Statistics of Extremes. Columbia Univ Press, NYC, NY

Haines WB (1930) Studies in the physical properties of soil: the hysteresis effect in capillary properties, and the modes of moisture distribution associated therewith. J Agri Sci 20:97–116

Hakkou R, Benzaazoua M, Bussière B (2008a) Acid mine drainage at the abandoned Kettara mine (Morocco): 1 environmental characterization. Mine Water Environ 27:145–159

Hakkou R, Benzaazoua M, Bussière B (2008b) Acid mine drainage at the abandoned Kettara mine (Morocco): 2 mine waste geochemical behavior. Mine Water Environ 27:160–170

Hakkou R, Benzaazoua M, Bussière B (2009) Laboratory evaluation of the use of alkaline phosphate wastes for the control of acidic mine drainage. Mine Water Environ 28(3):206–218

Hauser VL (2008) Evapotranspiration Covers for Landfills and Waste Sites. CRC Press, Boca Raton, FL

Haverkamp R, Reggiani P, Ross PJ, Parlange JY (2002) Soil water hysteresis prediction model based on theory and geometric scaling. Geophys Monogr 129:213–246

Hershfield DM (1965) Method for estimating probable maximum rainfall. J of the Am Waterworks Ass 57:965–972

Khire MV, Benson CH, Bosscher PJ (1999) Field data from a capillary barrier and model predictions with UNSAT-H. J Geotech and Geoenv Eng 125(6):518–527

Khire MV, Benson CH, Bosscher PJ (2000) Capillary barriers: design variables and water balance. J Geotech and Geoenv Eng 126:695–708

Kizito F, Campbell CS, Campbell GS, Cobos DR, Teare BL, Carter B, Hopmans JW (2008) Frequency, electrical conductivity and temperature analysis of a low-cost capacitance soil moisture sensor. J Hydrol 352:367–378

Koutsoyiannis D (1999) A probabilistic view of Hershfield's method for estimating probable maximum precipitation. Water Resour Res 35(4):1313–1322

Koutsoyiannis D (2003) On the appropriateness of the Gumbel distribution for modeling extreme rainfall. ESF LESC Exploratory Workshop, Hydro Risk, Bologna, Italy, http://itia.ntua.gr/getfile/590/1/documents/2003BolognaXtremrain.pdf

Lghoul M, Teixidó T, Pena JA, Hakkou R, Kchikach A, Guérin R, Jaffal M, Zouhri L (2012) Electrical and seismic tomography used to image the structure of a tailings pond at the abandoned Kettara mine, Morocco. Mine Water Environ 31(1):53–61

Madalinski KL, Gratton DN, Weisman RJ (2003) Evapotranspiration covers: an innovative approach to remediate and close contaminated sites. Remediation 14(1):55–67

Malazian A, Hartsough P, Kamai T, Campbell GS, Cobos DR, Hopmans JW (2011) Evaluation of MPS-1 soil water potential sensor. J Hydrol 402:126–134

Maqsoud A, Bussière B, Aubertin M, Mbonimpa M (2012) Predicting hysteresis of the water retention curve from basic properties of granular soils. Geotech Geol Eng 30(5):1147–1159

Mbonimpa M, Aubertin M, Chapuis RP, Bussière B (2002) Practical pedotransfer functions for estimating the saturated hydraulic conductivity. Geotech Geol Eng 20:235–259

McCarthy DF (2007) Essentials of soil mechanics and foundations: basic geotechnics, 7th edn. Pearson Prentice Hall, Upper Saddle River, NJ

McGuire P, Andraski BJ, Archibald RE (2009) Case study of a full-scale evapotranspiration cover. J Geotech Geoenv Eng 135(3):316–332

Merkus HG (2009) Particle Size Measurements: Fundamentals, Practice, Quality. Springer Particle Technology Series 17, ISBN: 978-1-4020-9015-8

Miller EE, Miller RD (1956) Physical theory for capillary flow phenomena. J Appl Phys 27:324–332

Morel-Seytoux H (1992) L'effet de barrière capillaire à l'interface de deux couches de sol aux propriétés fort contrastées. Hydrol Continent 7(2):117–128

Morris CE, Stormont JC (1997) Capillary barriers and subtitle D covers: estimating equivalency. J Env Eng 123(1):3–10

Mualem Y, Beriozkin A (2009) General scaling rules of the hysteretic water retention function based on Mualem's domain theory. Eur J Soil Sci 60:652–661

Nicholson RV, Gillham RW, Cherry JA, Reardon EJ (1989) Reduction of acid generation in mine tailings through the use of moisture-retaining cover layers as oxygen barriers. Can Geotech J 26:1–18

Nyhan JW (2005) Seven-year water balance study of an evapotranspiration landfill cover varying in slope for semiarid regions. Vadose Zone J 4:466–480

O'Kane M, Porterfield D, Endersby M, Haug MD (1998) The design and implementation of the field test plots at BHP Iron Ore, Mt Whaleback—a cover system for an arid climate. Preprint 98–70, SME, Littleton, CO, USA

O'Kane M, Porterfield D, Weir A, Watkins L (2000) Cover system performance in a semi-arid climate on horizontal and slope waste rock surfaces. Proc, International Conf on Acid Rock Drainage (ICARD) 2:1309–1318, Denver, CO, USA, ISBN: 0-87335-182-7

Papalexiou SM, Koutsoyiannis D (2006) A probabilistic approach to the concept of probable maximum precipitation. Adv Geosci 7:51–54

Poulovassilis A (1962) Hysteresis of pore water, an application of concept of independent domains. Soil Sci 93:405–412

Rock S, Myers B, Fiedler L (2012) Evapotranspiration (ET) Covers. Inter J of Phyto 14(S1):1–25

Ross B (1990) The diversion capacity of capillary barriers. Water Resour Res 26(10):2625–2629

Sanaa D, Zahraoui M, El Wartiti M, Jebrak M, Nahraoui FZ, Fadli D (2011) Environmental mining and sustainable development. Present Env Sustainable Development 5(2):17–21

Scanlon BR, Reedy RC, Keese KE, Dwyer SF (2005) Evaluation of evapotranspirative covers for waste containment in arid and semiarid regions in the southwestern. USA Vadose Zone J 4:55–71

Shackelford CD, Chang CK, Chiu TF (1994) The capillary barrier effect in unsaturated flow through soil barriers. Proc, 1st International Congr on Environmental Geotechnology, Edmonton, Canada, ISSMFE/CGS, pp 789–793

Smesrud JK, Benson CH, Albright WH, Richards JH, Wright S, Israel T, Goodrich K (2012) Alternative cover design in Northern California. Inter J Phyto 14(1):76–93

Steenhuis TS, Parlange JY, Kung KJS (1991) Comment on "the diversion capacity of capillary barriers" by B Ross. Water Resources Res 27:2155–2156

Stormont JC (1997) Incorporating capillary barriers in surface cover systems. Proc, Landfill Capping in the Semi-arid West, Grand Teton National Park, WY, USA, pp 39–51

Stormont JC, Anderson C (1999) Capillary barrier effect from underlying coarser layer. J Geotech Geoenv Eng 125(8):641–648

Stormont JC, Morris CE (1998) Method to estimate water storage capacity of capillary barriers. J of Geotech and Geoenv Eng 124(4):297–302

Van Genuchten MT (1980) A closed form equation for predicting the hydraulic conductivity of unsaturated soils. Soil Sci Soc Am J 44:892–898

Waugh WJ, Kastens MK, Sheader LRL, Benson CH, Albright WH, Mushovic PS (2008) Monitoring the performance of an alternative landfill cover at the Monticello, Utah, uranium mill tailings disposal site. Waste Management Conf, Phoenix, AZ, pp 24–28

Wels C, Fortin S, Loudon S (2002) Assessment of store and release cover for Questa tailings facility, New Mexico. Proc, 9th International Conf on Tailings and Mine Waste, Vail, CO, USA, pp 459–468

Williams DJ, Stolberg DJ, Currey NA (2006) Long-term monitoring of Kidston's « Store/Release » cover system over potentially acid forming waste rock piles. Proc, 7th ICARD, St Louis, MO, USA, pp 26-30

WMO (World Meteorological Organization) (1986) Manual for estimating of probable maximum precipitation. Operational hydrology report 1, 2nd edn, Publ 332, World Meteorological Org, Geneva, Switzerland

Zhan G, Aubertin M, Mayer A, Burke H, McMullen J (2001) Capillary cover design for leach pad closure. Proc, SME Annual Mtg, Denver, CO, USA, pp 1–9

Zhan G, Schafer W, Milczarek M, Myers K, Giraudo J, Espell R (2006) The evolution of evapotranspiration cover systems at Barrick Goldstrick Mines. 7th ICARD, St. Louis, MO, USA, pp 2585–2603